



Gibberellic acid as green corrosion inhibitor for carbon steel in hydrochloric acid solutions

A.S. Fouda*, G.Y. Elewady, K. Shalabi, S. Habbouba

Department of Chemistry, Faculty of Science, El-Mansoura University, El-Mansoura 35516, Egypt,

Received 14 Nov 2013, Revised 14 Feb 2014, Accepted 14 Feb 2014
email: asfouda@hotmail.com, Fax: +20502246254, Tel: +20502365730

Abstract

The inhibitive action of Gibberellic acid on the corrosion of carbon steel in 1 M HCl solution was investigated by weight loss, potentiodynamic polarization, electrochemical impedance spectroscopy (EIS) and electrochemical frequency modulations (EFM) techniques. Potentiodynamic polarization studies clearly reveal that Gibberellic acid acts essentially as mixed inhibitor. The inhibition efficiency was found to increase with inhibitor concentration. The adsorption of Gibberellic acid on carbon steel surface is found to obey Langmuir adsorption isotherm. The morphology of inhibited carbon steel was analyzed by scanning electron microscope (SEM) and energy dispersive X-ray spectroscopy (EDX). The mechanism of inhibition process was discussed in terms of the adsorption of Gibberellic acid on the metal surface.

Keywords: Corrosion inhibition; carbon steel; HCl; EFM; EIS; SEM; EDX.

1. Introduction

Hydrochloric acid (HCl) solutions are widely used for acid cleaning, industry acid pickling, oil well acidizing and acid decaling (1–4). The study of carbon steel corrosion phenomena has become important particularly in acidic media because of the increased industrial applications of acid solutions. Carbon steel has been widely employed as a construction material for pipe work in the oil and gas production, such as down holetubular, flow lines and transmission pipelines (5–15).

Different organic and non-organic compounds have been studied as inhibitors to protect metals from corrosion attack. Usually, organic compounds that exert a significant influence on the extent of adsorption on the metal surface and therefore can be used as effective corrosion inhibitors. The efficiency of these organic corrosion inhibitors is related to the presence of polar functions with S, O or N atoms in the molecule, heterocyclic compounds and π -electrons (16–21). The polar function is usually regarded as the reaction center for the establishment of the adsorption process (22). Such compounds can adsorb onto the metal surface and block the active surface sites, thus reducing the corrosion rate. Most of the natural products are nontoxic, biodegradable and readily available in plenty. Various parts of the plants, seeds (23, 24), fruits (25), leaves (26–28), and flowers (29–31) were extracted and used as corrosion inhibitors.

In the present work, chemical and electrochemical techniques were used to investigate the inhibition of carbon steel corrosion by 1 M HCl solution with respect to the effects of inhibitor concentration and temperature on the inhibitor efficiency (% IE).

2. Experimental details

2.1. Materials and solutions

Corrosion tests have been carried out on electrodes cut from sheets of carbon steel with composition (weight %): 0.36 C, 0.66 Mn, 0.27 Si, 0.02 S, 0.015 P, 0.21 Cr, 0.02 Mo, 0.22 Cu, 0.06 and the remainder iron. The specimens were embedded in epoxy resin leaving a working area of 1 cm. The working surface was subsequently ground up to 1200 grit size, washed by bidistilled water and acetone. The solutions (1 M HCl) were prepared by dilution of an analytical reagent grade 36% HCl with distilled water. All the tests were performed at ambient temperature (25°C). Gibberellic acid was purchased from Aldrich-Sigma Company.

2.2. Weight-loss measurements

The carbon steel specimens were polished with SiC emery papers (up to 1200 grit size), rinsed in bidistilled water and acetone, dried in a desiccator, weighed by an analytical balance (0.0001 g), and immersed in the test solutions for 30 min at different temperatures (298–318 K). Then the specimens were removed, washed by bidistilled water, dried between filter

papers, and weighed again. The difference of specimen weight before and after the immersion is the weight loss. The inhibition efficiency IE and the degree of surface coverage (θ) were calculated from equation (1):

$$\% \text{ IE} = \theta \times 100 = [1 - (W_1/W_2)] \times 100 \quad (1)$$

where W_1 and W_2 are the weight loss of the of carbon steel in the presence and absence of inhibitor, respectively.

2.3 Electrochemical measurement

A three-electrode cell including a working electrode, an auxiliary electrode and a reference electrode was used for the electrochemical measurements. The working electrodes were made of carbon steel sheets which were embedded in PVC holder using epoxy resin with a square surface of 1 cm^2 . The auxiliary electrode was a platinum foil, the reference electrode was a saturated calomel electrode (SCE) with a fine Luggin capillary tube positioned close to the working electrode surface in order to minimize ohmic potential drop (IR). Each specimen was successive abraded by using SiC emery papers up to 1200 grit size, washed with bidistilled water and degreased in acetone then dried between filter papers. The working electrode was immersed in the test solution at open circuit potential for 30 min before measurement until a steady state reached. Tafel polarization curves were determined by polarizing to $\pm 250 \text{ mV}$ with respect to the free corrosion potential (E vs. SCE) at a scan rate of 0.5 mV/s . Stern-Geary method (23) used for the determination of corrosion current is performed by extrapolation of anodic and cathodic Tafel lines to a point which gives $\log i_{\text{corr}}$ and the corresponding corrosion potential (E_{corr}) for inhibitor free acid and for each concentration of inhibitor. Then i_{corr} was used for calculation of inhibition efficiency (% IE) and surface coverage (θ) as in equation 2:

$$\% \text{ IE} = \theta \times 100 = [1 - (i_{\text{corr}}(\text{inh}) / i_{\text{corr}}(\text{free}))] \times 100 \quad (2)$$

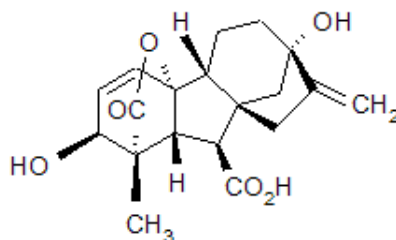
where $i_{\text{corr}}(\text{free})$ and $i_{\text{corr}}(\text{inh})$ are the corrosion current densities in the absence and presence of inhibitor, respectively.

EIS measurements were carried out in a frequency range of 100 kHz to 100 mHz with amplitude of 5 mV peak-to-peak. The experimental impedance was analyzed and interpreted based on the equivalent circuit. The main parameters deduced from the analysis of Nyquist diagram are the charge transfer resistance R_{ct} (diameter of high-frequency loop) and the double layer capacity C_{dl} . The inhibition efficiencies and the surface coverage (θ) obtained from the impedance measurements are calculated from equation 3:

$$\% \text{ IE} = \theta \times 100 = [1 - (R_{\text{ct}}^{\circ} / R_{\text{ct}})] \times 100 \quad (3)$$

where R_{ct}° and R_{ct} are the charge transfer resistance in the absence and presence of inhibitor, respectively.

All electrochemical measurements were carried out using Gamry Potentiostat/Galvanostat / ZRA (model PCI4/G750) with a Gamry framework system based on ESA400. Gamry applications include software EIS 300 for EIS measurements, DC 105 software for polarization and EFM 140 for EFM measurements; computer was used for collecting data. Echem Analyst 5.5 Software was used for plotting, graphing and fitting data. Each experiment was repeated at least three times to check the reproducibility. All tests have been performed in deaerated solutions under unstirred conditions at 25°C .



Formula: $\text{C}_{19}\text{H}_{22}\text{O}_6$, Molar mass: 346.37

Figure 1: Chemical structure, molecular formula and molar mass of the Gibberellic acid

2.4 Surface analysis

The specimens used for surface morphology examination were immersed in 1 M HCl in the absence (blank) and presence of 300 ppm of aqueous Gibberellic acid at 25°C for 3 hours. The analysis was performed using scanning electron microscope (JOEL 840, Japan).

3. Results and discussion

3.1. Weight loss measurements

Figure 1 represents weight loss-time curves of carbon steel in 1 M HCl in the absence and presence of different concentrations of Gibberellic acid at 25°C . The values of percentage inhibition efficiency (% IE) obtained for different concentrations and the corrosion rates of the inhibitor at 25°C are given in Table 1. From the data it can be seen that the corrosion rate decreases and the inhibition efficiency increases as the concentration of the inhibitor increases due to the adsorption of the inhibitor (32) on the metal surface.

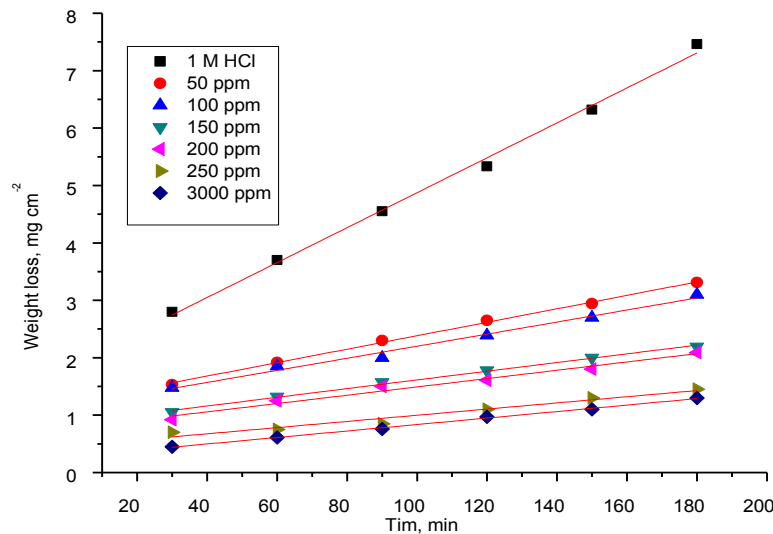


Figure 1: Weight loss-time curves of carbon steel in 1M HCl in the absence and presence of different concentrations of Gibberellic acid at 25°C.

Table 1: Data of weight loss measurements for carbon steel in 1M HCl solution in the absence and presence of different concentrations of Gibberellic acid 25°C.

Conc., ppm	C.R., (mg cm ⁻² min ⁻¹)	θ	% IE
0.00	0.0444	--	--
50	0.0220	0.502	50.2
100	0.0199	0.551	55.1
150	0.0148	0.666	66.6
200	0.0134	0.698	69.8
250	0.0085	0.808	80.8
300	0.0081	0.818	81.8

3.2 Electrochemical impedance spectroscopy measurements

The corrosion behaviour of carbon steel in 1 M HCl solution in the presence of Gibberellic acid was investigated by EIS at 25° C after 30 min of immersion. Figure 2 shows the results of EIS experiments in the Nyquist representation. After analyzing the shape of the Nyquist plots, it is concluded that the curves approximated by a single capacitive semi-circles, showing that the corrosion process was mainly charge transfer controlled (33). The general shape of the curves is very similar for all samples; the shape is maintained throughout the whole concentrations, indicating that almost no change in the corrosion mechanism occurred due to the inhibitor addition (34). The diameter of Nyquist plots (R_p) increases on increasing the Gibberellic acid concentration. These results suggest the inhibition behaviour of Gibberellic acid on corrosion of carbon steel in 1 M HCl solution.

The Nyquist plots are analyzed in terms of the equivalent circuit composed with classic parallel capacitor and resistor (shown in Figure 3) (35). The impedance of a CPE is described by the equation 4:

$$Z_{CPE} = Y_0^{-1} (j\omega)^{-n} \quad (4)$$

where Y_0 is the magnitude of the CPE, j is an imaginary number, ω is the angular frequency at which the imaginary component of the impedance reaches its maximum values and n is the deviation parameter of the CPE: $-1 \leq n \leq 1$. The values of the interfacial capacitance C_{dl} can be calculated from CPE parameter values Y_0 and n using equation 5:

$$C_{dl} = Y (\omega_{max})^{n-1} \quad (5).$$

The impedance parameters including polarization resistance R_{ct} , double layer capacitance C_{dl} and inhibition efficiency % IE are given in Table 2.

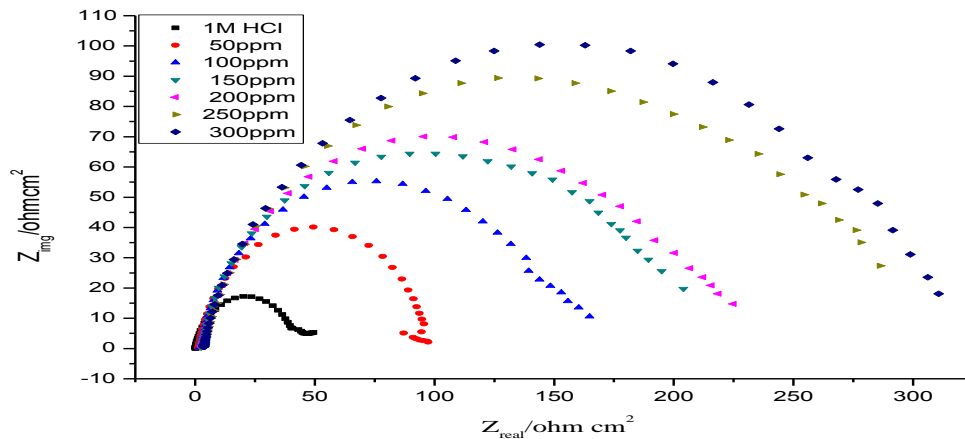


Figure 2: Nyquist plots for carbon steel in 1M HCl at different concentrations of Gibberellic acid.

It is clear that the value of R_{ct} increases on increasing the concentration of the inhibitor, indicating that the corrosion rate decreases in the presence of the inhibitor. It is also clear that the value of C_{dl} decreases on the addition of inhibitors, indicating a decrease in the local dielectric constant and/or an increase in the thickness of the electrical double layer, suggesting the inhibitor molecules function by the formation of the protective layer at the metal surface (36). Deviations from a perfect circular shape indicate frequency dispersion of interfacial impedance. This anomalous phenomenon is attributed in the literature to the no homogeneity of the electrode surface arising from the surface roughness or interfacial phenomena (37-39).

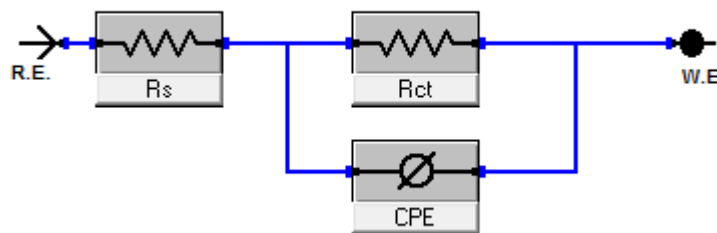


Figure 3.Electrical equivalent circuit used to fit the impedance data.

Table 2: EIS data of carbon steel in 1 M HCl and in the presence of different concentrations of Gibberellic acid at 25° C.

Conc., (ppm)	R_s Ohm cm^{-2}	n	R_{ct} Ohm cm^2	C_{dl} $\mu F cm^{-2}$	θ	% IE
0.00	1.21	0.854	45.1	345.8	--	--
50	1.48	0.876	93.7	170.1	0.518	51.8
100	2.20	0.848	143.1	168.2	0.684	68.4
150	2.30	0.815	185.0	120.2	0.756	75.6
200	2.90	0.815	192.1	112.1	0.764	76.4
250	2.80	0.782	275.2	107.1	0.836	83.6
300	3.30	0.803	277.2	104.2	0.837	83.7

3.3 Potentiodynamic polarization measurements

Figure 4 represents the anodic and cathodic polarization curves of carbon steel electrode, in 1 M HCl solutions containing different concentrations of Gibberellic acid. Inspection of Figure 1 reveals that, both anodic and cathodic polarization curves are shifted to less current density values in the presence of Gibberellic acid. This behavior suggests the inhibitive action of Gibberellic acid. The extent of the shift in current density increases with increasing of Gibberellic acid concentration. The values of corrosion current density (i_{corr}), corrosion potential (E_{corr}), anodic Tafel constants (β_a) and cathodic Tafel constant (β_c), excluded from polarization curves are given in **Table 3**.

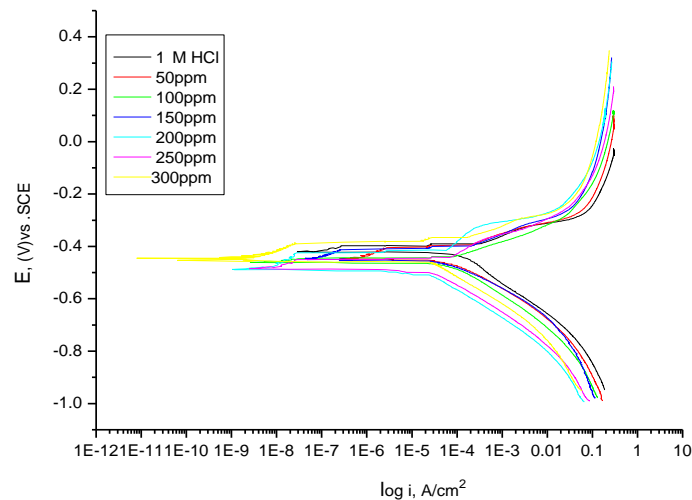


Figure 4: Potentiodynamic polarization for corrosion of carbon steel in 1 M HCl in the absence and presence of different concentrations of Gibberellic acid at 25°C.

Inspection of **Table 3** reveals that the corrosion potential of carbon steel in the acid solution is largely shifted to less negative values (noble direction) upon addition of Gibberellic acid. On the other hand, the corrosion current density is greatly reduced upon addition of Gibberellic acid. These results suggest the inhibitive effects of the Gibberellic acid. The data in Table 3 reveal that the values of inhibition efficiency obtained by polarization technique are comparable to those obtained by weight loss measurements and EIS. The inhibition efficiency increases with increasing Gibberellic acid concentration. Further inspection of **Table 3** reveals that the addition of increasing concentrations of Gibberellic acid decreases both the anodic and cathodic Tafel constants. This result indicates that the Gibberellic acid acts as mixed inhibitors (40). This means that the Gibberellic acid molecules are adsorbed on both the anodic and cathodic sites resulting in an inhibition of both anodic dissolution and cathodic reduction reactions. The greater the metal surface area occupied by adsorbed molecules, the higher the inhibition efficiency.

Table 3: Potentiodynamic data of carbon steel in 1 M HCl and in the presence of different concentrations of Gibberellic acid at 25 °C.

Conc (ppm)	$-E_{corr}$ mV vs SCE	I_{corr} , $\mu A\ cm^{-2}$	$-\beta_a$ mV dec ⁻¹	β_c mV dec ⁻¹	C.R. mmy ⁻¹	θ	IE%
0.00	456	2.6	44.8	25.0	164.1	--	--
50	444	2.1	27.1	24.0	71.0	0.192	19.2
100	460	1.9	25.1	24.1	38.9	0.269	26.9
150	464	0.27	28.4	28.4	20.8	0.896	89.6
200	486	0.27	20.1	25.1	15.3	0.896	89.6
250	484	0.053	24.5	30.1	12.2	0.980	98.0
300	446	0.012	30.8	32.2	11.0	0.995	99.5

3.4 Electrochemical frequency modulation (EFM) measurements

EFM is a nondestructive corrosion measurement like EIS a small signal technique. Unlike EIS, however, two sine waves (at different frequencies) are applied to the cell simultaneously. The great strength of the EFM is the causality factors which serve as an internal check on the validity of the EFM measurement (41). With the causality factors the experimental EFM data can be verified. Results of EFM experiments are a spectrum of current response as a function of frequency. The spectrum is called the intermediation spectrum. The spectra contain current responses assigned for harmonical and intermediation current peaks. The larger peaks were used to calculate the corrosion current density (i_{corr}), the Tafel slopes (β_a and β_c) and the causality factors (CF-2 and CF-3). Intermediation spectra obtained from EFM measurements are presented in **Figure 5** for 1 M HCl in absence and presence of Gibberellic acid. **Table 4** indicated that; the corrosion current densities decrease by increasing the concentrations of the studied inhibitors.

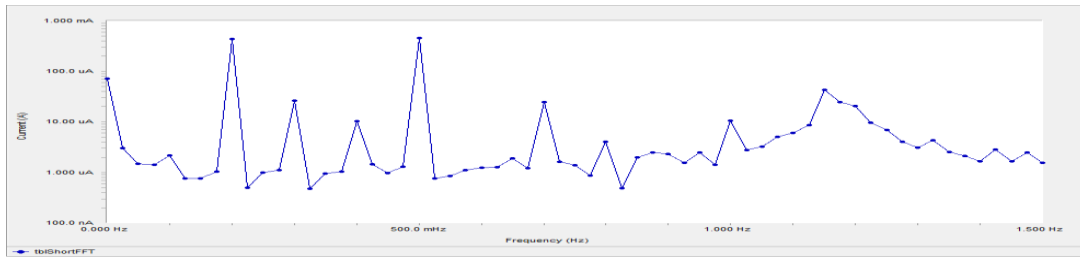


Figure 5: Intermediation spectra for carbon steel in 1 M HCl.

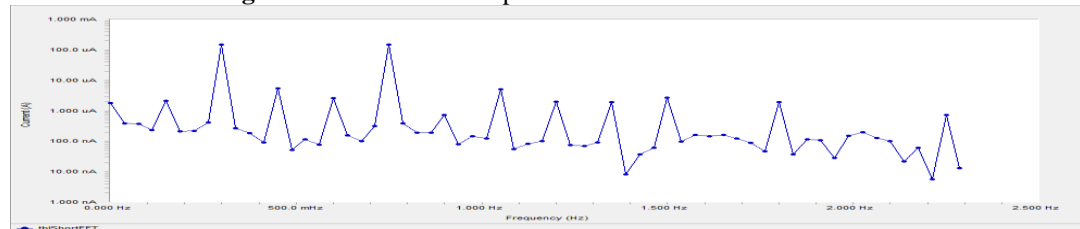


Figure 5: Intermediation spectra for carbon steel in 1 M HCl in the absence and presence of 50ppm.

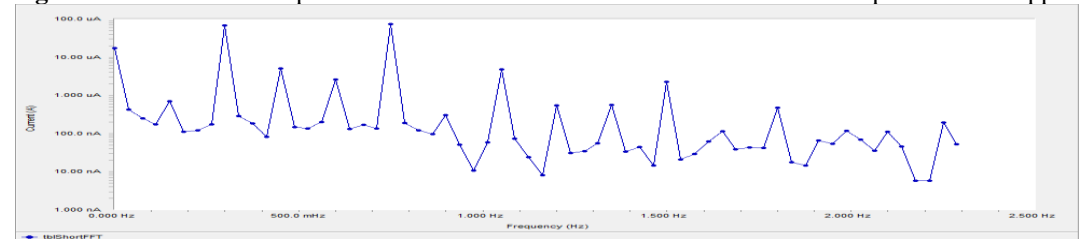


Figure 5: Intermediation spectra for carbon steel in 1 M HCl in the absence and presence of 100ppm.

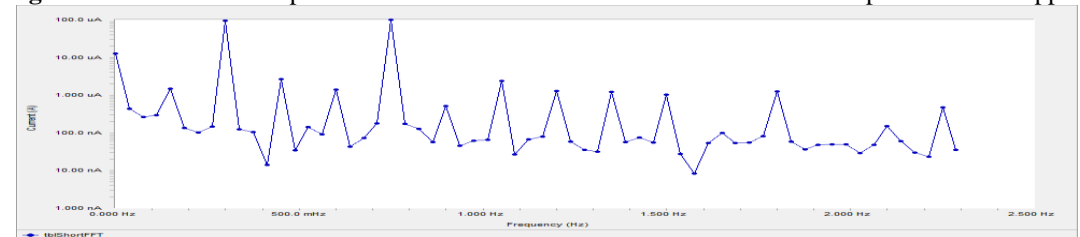


Figure 5: Intermediation spectra for carbon steel in 1 M HCl in the absence and presence of 150ppm.

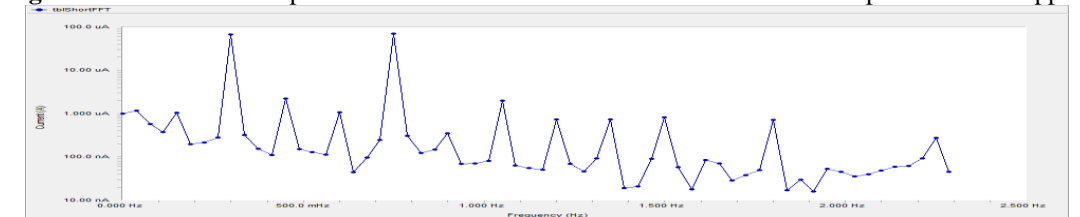


Figure 5: Intermediation spectra for carbon steel in 1 M HCl in the absence and presence of 200ppm.

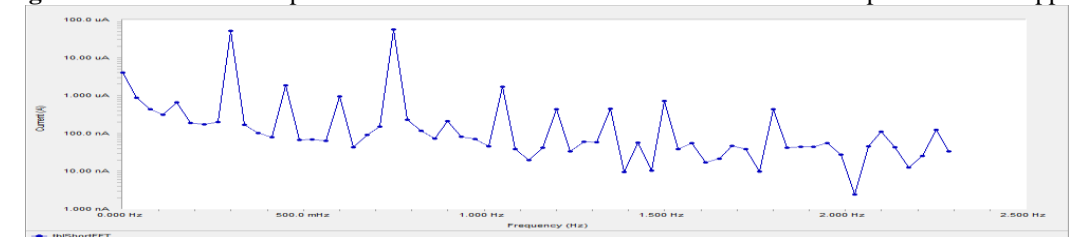


Figure 5: Intermediation spectra for carbon steel in 1 M HCl in the absence and presence of 250ppm.

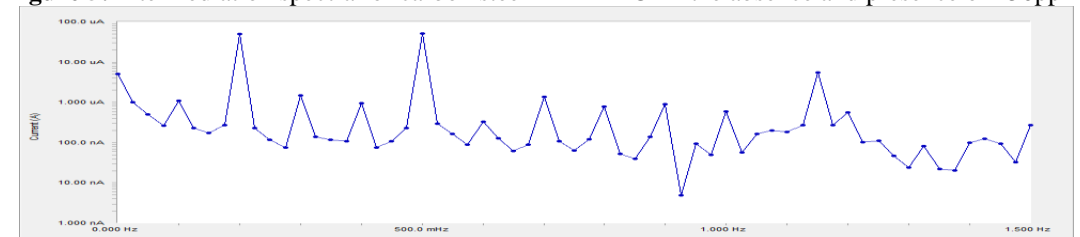


Figure 5: Intermediation spectra for carbon steel in 1 M HCl in the absence and presence of 300ppm.

Table 4: Electrochemical kinetic parameters obtained by EFM technique for carbon steel in the absence and presence of various concentrations of Gibberellic acid in 1 M HCl at 25 °C.

Conc	I_{corr} , $\mu A cm^{-2}$	β_a , $mV dec^{-1}$	β_c , $mV dec^{-1}$	CF-2	CF-3	C.R., $mm y^{-1}$	θ	IE $_{EFM}\%$
blank	650.0	80.7	112.1	2.4	3.2	297.0	-----	-----
50	230.4	113.1	91.2	1.99	2.7	113.9	0.649	64.9
100	157.5	111.0	212	2.01	2.6	71.9	0.758	75.8
150	149.3	92.6	108.3	2.03	2.6	68.2	0.770	77.0
200	113.5	97.0	120.0	2.02	2.5	51.8	0.825	82.5
250	101.6	109.0	140.8	2.01	2.9	46.6	0.843	84.3
300	69.2	83.0	97.6	1.8	2.7	31.6	0.893	89.3

3.5. Adsorption isotherm

The adsorption process depends on the electronic characteristics of the inhibitor, the nature of metal surface, temperature, stric effects and the varying degrees of surface-site activity (42).The establishment of isotherms that describe the adsorption behavior of corrosion inhibitor is important as they provide important clues about the nature of metal-inhibitor interactionThe simplest isotherm equation is Langmuir:

$$C/\theta = 1/K_{ads} + C \tag{6}$$

where K_{ads} the binding constant of the adsorption reaction and C is the inhibitor concentration in the bulk of the solution.Plots of C/θ vs. C(Langmuir adsorption plots) yielded straightlines.The intercept of each straight line was equal to the reciprocal the binding constant (Figure 6).Values of the binding constants are listed in Table 5. The higher values of the binding constant indicated higher adsorption of the Gibberellic acid on the carbon steel surface in 1 M HCl solution.

Standard free energy (ΔG°_{ads})was obtained according to the following equation (43):

$$\Delta G^{\circ}_{ads} = - RT \ln(55.5K_{ads}) \tag{7}$$

where 55.5 is the concentration of water in solution expressed in $g^{-1}L$.The calculated values of ΔG°_{ads} were listed in Table 5.

Table 5: Values of adsorption parameters of Gibberellic acid at 25°C.

Inhibitor	Temp.,K	Ads. isotherm	K_{ads} , $g^{-1}L$	slope	$-\Delta G^{\circ}_{ads}$, kJ mol
Gabbirellic acid	326	Langmuir	30.3	1.1	20.2

As can be seen from Table 5, ΔG°_{ads} also decreases with increasing temperature. Generally speaking, values of ΔG°_{ads} up to $-20 kJ mol^{-1}$ are consistent with the electrostatic interaction between the charged molecules and the charged metal (physical adsorption) while those more negative than $-40 kJ mol^{-1}$ involve sharing or transfer of electrons from the inhibitor molecules to the metal surface to form a co-ordinate type of bond (chemisorptions) (44). In the case of this study, the value of ΔG°_{ads} is about $20.2 kJ mol^{-1}$, this may indicate that both physical and chemical adsorptions took place (45).

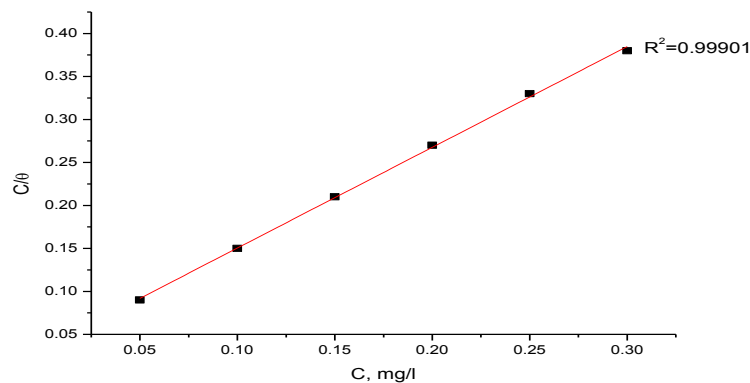


Figure 6: Langmuir adsorption plots for carbon steel in 1 M HCl containing various concentrations of Gibberellic acid.

3.6 Effect of temperature

Temperature plays an important role on the progress of the corrosion reactions of carbon steel in HCl solutions. Increasing the temperature increases the energy of the reactants to form the activated complex which dissociates to yield the corrosion products (46).The corrosion rates of carbon steel were calculated at 25°C-45°C in the

absence and the presence of the Gibberellic acid. Activation energies (E_a^*) for the corrosion of carbon steel in the absence and presence of different concentrations of Gibberellic acid were calculated using Arrhenius-type equation (47):

$$\text{(Rate) } k = A \exp(-E_a^*/RT) \quad (8)$$

where k is the corrosion rate, A is a constant depends on a metal type and electrolyte and E_a^* is the apparent activation energy. Arrhenius plots for the corrosion rate of carbon steel in 1 M HCl are shown in Figure 7. Values of E_a^* for carbon steel in 1 M HCl in the absence and presence of different concentrations of Gibberellic acid were calculated from the slope of $\log k$ versus $1/T$ plots and are given in Table 6. From the results of this Table, it is seen that the inhibition efficiency of the Gibberellic acid decreases with increase in temperature (48) suggesting physisorption. This may be due to the desorption of the inhibitor molecules (49) from the metal surface at higher temperatures.

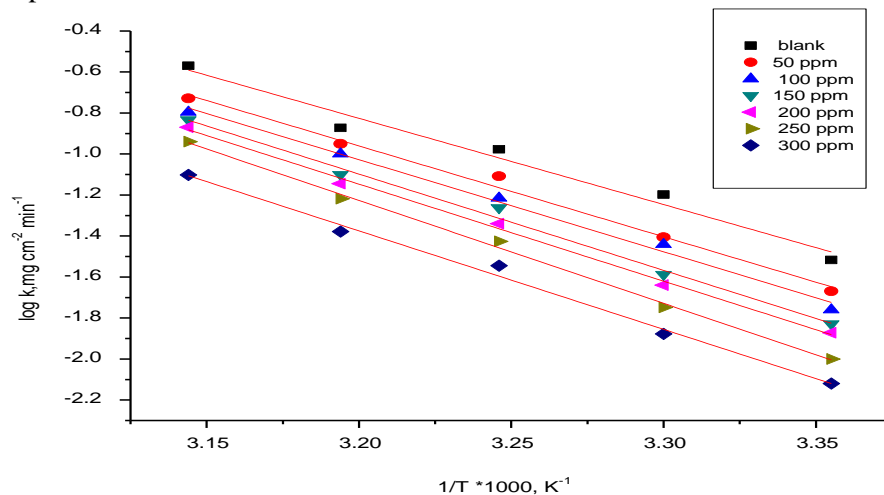


Figure 7: $\log k$ (corrosion rate) – $1/T$ curves for for carbon steel in 1 M HCl in the absence and presence of different concentrations of Gibberellic acid.

The enthalpy of activation (ΔH^*) and entropy of activation (ΔS_a^*) for the corrosion of carbon steel in HCl were obtained by applying the transition-state equation (50):

$$\text{Rate (k)} = RT/Nh \exp(\Delta S^*/R) \exp(-\Delta H^*/RT) \quad (9)$$

where h is Planck's constant, N is Avogadro's number, ΔH^* is the activation enthalpy and ΔS^* is the activation entropy. A plot of $\log(\log k/T)$ versus $1/T$ for carbon steel in 1 M HCl in the absence and presence of different concentrations of Gibberellic acid gives straight lines as shown in Figure 8.

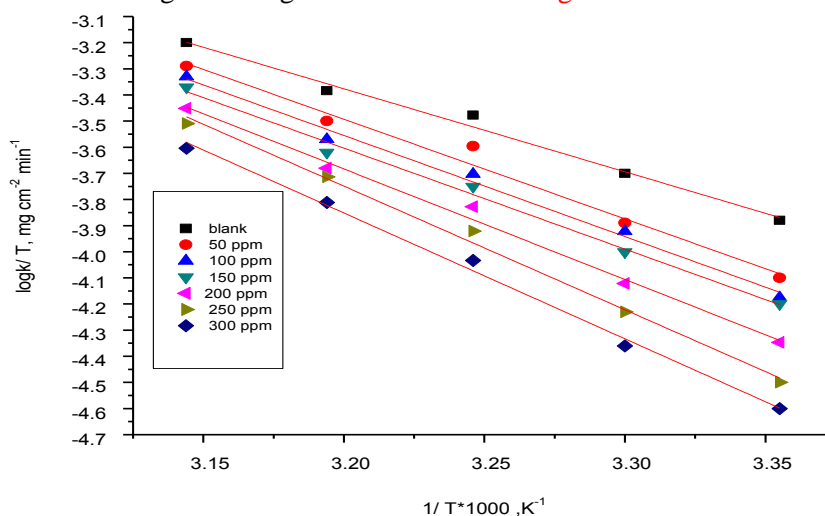


Figure 8: $\log k$ (corrosion rate)/ T – $1/T$ curves for for carbon steel in 1 M HCl in the absence and presence of different concentrations of Gibberellic acid.

These values (Table 6) indicate that the presence of the Gibberellic acid increases the activation energy, E_a^* and the activation enthalpy, ΔH^* and decreases the activation entropy, ΔS^* for the corrosion process. It is obviously that

the activation energy strongly increases in the presence of inhibitors; this result was attributed to the inhibitors species being physically adsorbed on the carbon steel surface (51-53). The higher activation energy for inhibitors as compared to that of free acid may be explained according to Riggs and Hurd (54), as they stated that at higher levels of surface coverage the corrosion process may proceed on the adsorbed layer of inhibitor and not on the metal surface leading to a decrease in the apparent activation energy. The results showed the positive signs for ΔH^* reflecting the endothermic nature of the corrosion process. The increase in the activation enthalpy (ΔH^*) in presence of the inhibitors implies that the addition of the inhibitors to the acid solution increases the height of the energy barrier of the corrosion reaction to an extent depends on the type and concentration of the present inhibitor. The negative values of ΔS^* pointed to a greater order produced during the process of activation. This can be achieved by the formation of an activated complex representing an association or fixation with consequent loss in the degrees of freedom of the system during the process (55).

Table 6: Activation parameters for dissolution of carbon steel the absence and presence of different concentrations of Gibberellic acid in 1 M HCl.

Conc	E^*_a , kJ mol ⁻¹	ΔH^* , kJ mol ⁻¹	ΔS^* , Jmol ⁻¹	R^2
Blank	80.5	71.4	67.6	0.9974
50	84.4	72.9	30.9	0.9591
100	86.1	74.1	29.1	0.9353
150	89.9	74.0	30.9	0.9368
200	90.7	76.6	9.9	0.9314
250	95.1	89.9	-13.1	0.9936
300	92.1	91.1	-22.6	0.9987

3.7. SEM studies

A photograph of the polished carbon steel surface before immersion in 1M HCl solution is shown in **Figure 9a**.

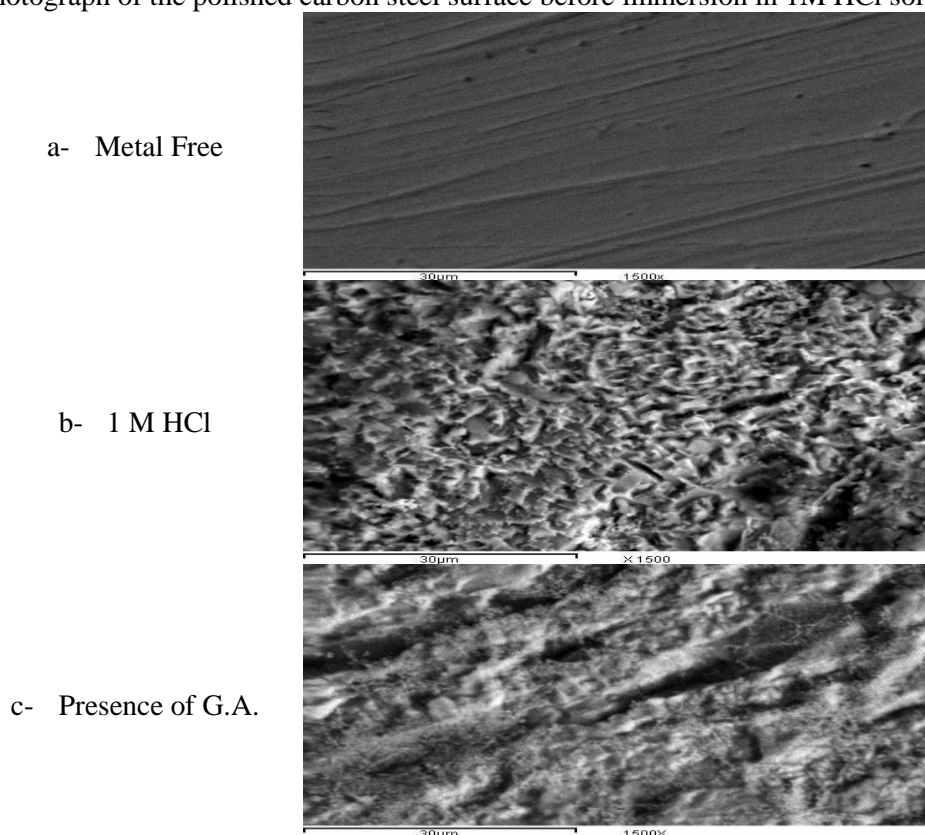


Figure 9: SEM micrographs of carbon steel surface (a) before of immersion in 1 M HCl, (b) after 3 h of immersion in 1 M HCl and (c) after 3 h of immersion in 1 M HCl + 300 ppm of Gibberellic acid at 25 °C

The photograph shows the surface was smooth and without pits. A photograph of the carbon steel surface after immersion in 1 M HCl solution is shown in **Figure 9b**. The photograph revealed that, the surface was strongly damaged in the absence of Gibberellic acid. A photograph of the carbon steel surface after immersion in 1 M HCl

solution containing 300 ppm of Gibberellic acid is shown in Figure 9c. It was found that the faceting observed in figures disappeared and the surface was free from pits and it was smooth. It can be concluded from Figure 9c that corrosion decreased largely in the presence of Gibberellic acid and hence corrosion was inhibited strongly when Gibberellic acid was present in the medium

Figures 10(a)–10(c) show the EDX spectrum in the absence and presence of Gibberellic acid. In the presence of Gibberellic acid., Figures 9(b) and 9(c), EDX spectra show an additional line characteristic for the existence of N. In addition, the intensities of C, and O signals are enhanced. The appearance of the N signal and this enhancement in the C and O signals is due to the N, C and O atoms constituting the Gibberellic acid. which indicate that the inhibitor molecules have adsorbed on the metal surface. Data obtained from the spectra are presented in Table 7. The spectra show also that Fe peaks are considerably suppressed in the presence of inhibitor which is due to the overlying inhibitor film. These results confirm those from electrochemical measurements which suggest that a surface film inhibits the metal dissolution, and hence retarded the hydrogen evolution reaction (56, 57). EDX spectrum displays the characteristic peaks (F, O and Cl) ascribed to general corrosion in diluted hydrochloric acid.

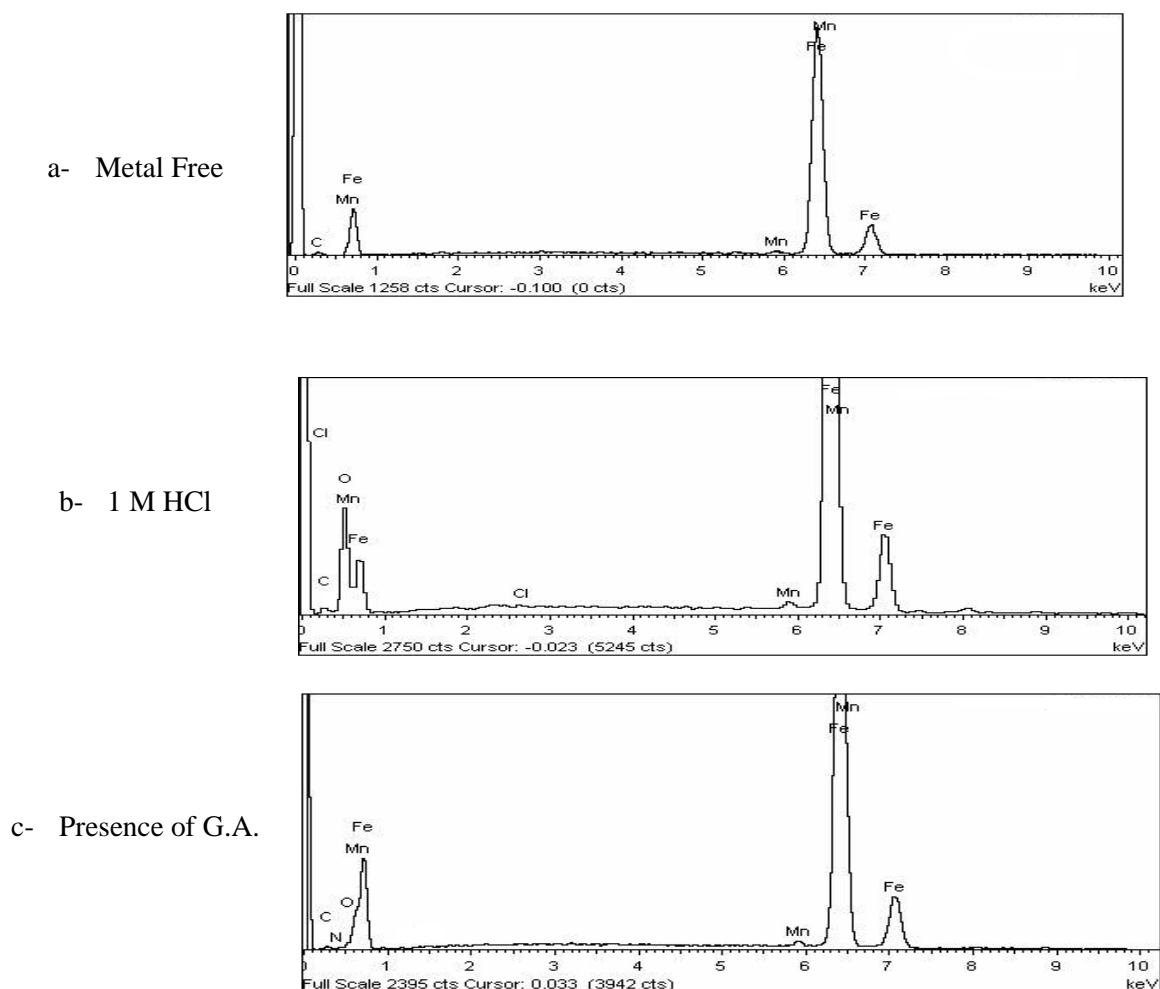


Figure 10: EDX spectra of carbon steel surface: (a) before of immersion in 1 M HCl, (b) after 3 h of immersion in 1 M HCl and (c) after 3 h of immersion in 1 M HCl + 300 ppm Gibberellic acid at 25 °C.

Table 7: Surface composition (wt %) of carbon steel before and after immersion in 1 M HCl without and with 300 ppm of Gibberellic acid at 25 °C.

(Mass %)	Fe	Mn	C	O	N	Cl
Pure	94.52	0.61	4.87	-	-	-
blank	57.83	0.31	2.12	39.42	-	0.32
G.A	63.33	0.51	16.23	15.12	4.81	-

3.7 Mechanism of inhibition:

Results of the present study have shown that Gibberellic acid inhibits the acid induced corrosion of carbon steel by virtue of adsorption of it onto the metal surface. The inhibition process is a function of the metal, inhibitor concentration, and temperature as well as inhibitor adsorption abilities which is so much dependent on the number of adsorption sites. The mode of adsorption (physiosorption and chemisorption) observed could be attributed to the fact that Gibberellic acid contains many different donating atoms which some can adsorb chemically and others adsorb physically. This observation may be attributed to the fact that adsorbed organic molecules can influence the behavior of electrochemical reactions involved in corrosion processes in several ways. The action of organic inhibitors depends on the type of interactions between the substance and the metallic surface. The interactions can bring about a change either in electrochemical mechanism or in the surface available for the processes (58).

Gibberellic acid molecules may also be adsorbed via donor-acceptor interactions between the unshared electron pairs of the heteroatom's (O) to form a bond with the vacant d-orbitals of the iron atom on the metal surface, which act as a Lewis acid, leading to the formation of a protective chemisorbed film (59). In acidic solution, therefore the positively charged surface sites will electrostatically attract any anions present in solution, and repel cations. Gibberellic acid may adsorb on the carbon steel surface in two different adsorption types: (a) electrostatic interaction between a negatively charged surface, which is provided with specifically adsorbed anions (Cl^-) on carbon steel and the positive charge of the inhibitor (in case of pretention of the inhibitor), (b) interaction of unshared electron pairs in the molecule (present in oxygen) with carbon steel surface, atoms (60).

Conclusions

On the basis of this study the following conclusions can be drawn:

- (1) The Gibberellic acid acts as inhibitor for carbon steel corrosion in acidic medium.
- (2) Inhibition efficiency of Gibberellic acid increases with increase in concentration of the inhibitor and also with decrease in temperature.
- (3) The corrosion inhibition is probably due to the adsorption of the Gibberellic acid on the metal surface and blocking its active sites by phenomenon of physical and chemical adsorption.
- (4) The Gibberellic acid was found to obey Langmuir adsorption isotherm from the fit of the experimental data at all the concentrations studied.
- (5) The values of E_a^* obtained in the presence of the Gibberellic acid were higher compared to the blank acid solution which further support the physical adsorption proposed.
- (6) The values of ΔG_{ads}^0 obtained are low and negative, which reveals the spontaneity of the adsorption process.
- (7) SEM reveals the formation of a smooth surface on carbon steel in presence of Gibberellic acid probably due to the formation of an adsorptive film of electrostatic character.

References

1. Li L.F.; Caenen P.; Celis J.P., *Corros. Sci.* 50 (2008) 804.
2. El Ouali I., Hammouti B., Aouniti A., Ramli Y., Azougagh M., Essassi E.M., Bouachrine M. *J. Mater. Environ. Sci.* 1 (2010) 1
3. Karakus M.; Sahin, M.; Bilgic, S., *Mater. Chem. Phys.* 92 (2005) 565.
4. Sherif E.M.; Park, S.M., *Electrochim. Acta* 51 (2006) 4665
5. Jiang X.; Zheng, Y.G.; Qu, D.R.; Ke, W., *Corros. Sci.*, 48 (2006) 3091
6. Villamizar W.; Casales, M.; Gonzalez-Rodriguez, J.G.; L., Martinez CO., *Journal of Solid State Electrochemistry*, 11 (2007) 619.
7. Papavinasam S.; Doiron, A.; Panneerselvam, T.; Revie, R.W., *Corrosion* 63 (2007) 704.
8. Modiano S.; Fugivara, C.S.; Benedetti, A.V., *Corros. Sci.* 46 (2004) 529.
9. Migahed M.A., *Progress in Organic Coatings* 54 (2005) 91.
10. Deyab M.A., *Corros. Sci.* 49 (2007) 2315.
11. Knag M.; Sjoblom, J., *Journal of Dispersion Science and Technology* 27 (2006) 65.
12. Abdallah M.; Helal, E.A.; Fouda, A.S., *Corros. Sci.* 48 (2006) 1639.
13. Smith L., *British Corrosion Journal* 34 (1999) 247.
14. Petersen A.G.; Klenerman, D.; Hedges, W.M., *Corrosion* 60 (2004) 187.
15. Turnbull A.; Coleman, D.; Griffiths, A.J.; Francis, P.E.; Orkney, L., *Corrosion* 59 (2003) 250.
16. Quraishi M.A.; Jamal, D., *J. Appl. Electrochem.* 32 (2002) 425.
17. Elayyachy M.; El Idrissi, A.; Hammouti, B., *Corros. Sci.* 48 (2006) 2470.
18. Emregül K.C.; Hayvad, M., *Corros. Sci.* 48 (2006) 797.
19. Mernari B.; Elattari, H.; Traisnel, M.; Bentiss, F.; Lagrenee, M., *Corros. Sci.* 40 (1998) 391.

20. Wang L., *Corros. Sci.* 43 (2001) 2281.
21. Azhar M.E.; Mernari, M.; Traisnel, M.; Bentiss, F.; Lagrenee, M., *Corros. Sci.* 43 (2001) 2229.
22. Roberge P.R., *Corrosion inhibitors, Handbook of Corrosion Engineering*, McGraw-Hill, New York, 1999.
23. Saleh R.M.; Ismail, A.A.; El Hosary, A.A., *Corros. Sci.* 23 (1983) 1239.
24. Zucchi F.; Omar, I.H.; *Surf. Technol.* 24 (1985) 391.
25. Farooqi I.H.; Quraishi, M.A.; Saini, P.A., *Corros. Prev. Control* 46 (1999) 93.
26. Leelavathi S.; Rajalakshmi R., *J. Mater. Environ. Sci.* 4 (2013) 625-638.
27. Shivakumar S.S.; Mohana K.N., *J. Mater. Environ. Sci.* 4 (2013) 448-459.
28. Kliškić M.; Radošević, J.; Gudic, S.; Katalinic, V., *J. Appl. Electrochem.* 30 (2000) 823.
29. Minhaj A.; Saini, P.A.; Quraishi, M.A.; Farooqi, I.H., *Corros. Prev. Control* 46 (1999) 32.
30. Srivastava K.; Srivastava, P., *Corros. Prev. Control* 27 (1980) 5.
31. Saleh R.M.; Ismail, A.A.; El Hosary, A.A., *Corros. Prev. Control* 31 (1984) 21.
32. Obot I. B., *Int. J. Electrochem. Sci.* 4 (2009) 1277.
33. Rosliza R.; Wan Nik, W.B.; Senin, H.B., *Mater. Chem. Phys.* 107 (2008) 281.
34. Reide F.M.; Melo, H.G.; Costa, I., *Electrochim. Acta* 51 (2006) 1780.
35. Abdel-Gaber M.; Abd-El-Nabey, B.A.; Sidahmed, I.M.; El-Zayaday, A.M.; Saadawy, M., *Corros. Sci.* 48 (2006) 2765.
36. Ostovari A.; Hoseinie, S.M.; Peikari, M.; Shadizadeh, S.R.; Hashemi, S.J., *Corros. Sci.* 51 (2009) 1935.
37. Quraishi M.A.; Farooqi, I.H.; Saini, P.A., *Corrosion* 55 (1999) 493.
38. Raja P.B.; Sethuraman, M.G., *Mater. Lett.* 62 (2008) 2977.
39. Abdel-Gaber A.M.; Abd-El-Nabey, B.A.; Saadawy, M., *Corros. Sci.* 51 (2009) 1038.
40. de Souza F.S.; Spinelli, A., *Corros. Sci.* 51 (2009) 642.
41. Negm N.A.; Zaki, M.F., *J. Colloid Surf. A: Physicochem. Eng. Aspec.* 322 (2008) 97.
42. Donahue F.M.; Nobe, K., *J. Electrochem. Soc.* 112 (1965) 886.
43. El-Awady A.A.; Abd-El-Nabey, B.A.; Aziz, S.G., *J. Electrochem. Soc.* 139 (1992) 2149.
44. El-Etre A.Y.; *J. Colloid Interface Sci.* 314 (2007) 578.
45. Quartarone G.; Battilana, M.; Bonaldo, L.; Tortato, T., *Corros. Sci.* 50 (2008) 3474.
46. Badawy W.A.; Ismail, K.M.; Fathi, A.M., *Electrochim. Acta* 51 (2006) 4182.
47. F. Bentiss M. Lebrini, M. Lagrenee, *Corros. Sci.* 47 (2005) 2915.
48. Elewady G. Y.; El-Said, I. A.; Fouda, A. S., *Int. J. Electrochem. Sci.* 3 (2008) 644.
49. Oguzie E., *Portugaliae Electrchimica Acta*, 26 (2008) 303.
50. Putilova I.N.; Balezin, S.A.; Barannik, V.P., *Metallic Corrosion Inhibitors*, Pergamon Press, New York, 1960, pp. 31.
51. Almeida C.M.V.B.; Raboczkay, T.; Griannetti, B.F., *J. Appl. Electrochem.* 29 (1999) 123.
52. Bentiss F.; Lebrini, M.; Lagrenee, M., *Corros. Sci.* 47 (2005) 2915.
53. Mora N.; Cano, E.; Polo, J.L.; Puente, J.M.; Bastidas, J.M., *Corros. Sci.* 46 (2004) 563.
54. Riggs J.L.O.; Hurd, T.J., *Corrosion* 23 (1967) 252.
55. Bouklah M.; Hammouti, B.; Lagrenee, M.; Bentiss, F., *Corros. Sci.* 48 (2006) 2831.
56. Rehim S.S.A.; Hazzazi, O. A.; Amin, M. A.; Khaled, K. F., *Corros. Sci.* 50 (2008) 2258.
57. Fragoza-Mar L.; Olivares-Xometl, O.; Domnguez-Aguilar, M. A.; Flores, E. A.; Arellanes-Lozada P., Jimenez-Cruz, F., *Corros. Sci.* 61 (2012) 171.
58. Aramaki K.; Hackermann, N. J., *Electrochem. Soc.*, 116 (1969) 568.
59. Ahamad I., Quraishi, M.A., *Corros. Sci.* 52 (2010) 651.
60. Emregul K.C.; Atakol, O., *Mater. Chem. Phys.* 83 (2004) 373.